

# 2G HTS wire with enhanced engineering current density attained through the deposition of HTS layer with increased thickness

A. Markelov<sup>a,b</sup>, A. Valikov<sup>b</sup>, V. Chepikov<sup>b</sup>, A. Petrzhik<sup>b</sup>, B. Massalimov<sup>b</sup>,  
P. Degtyarenko<sup>a,c</sup>, R. Uzkih<sup>a</sup>, A. Soldatenko<sup>a,c</sup>, A. Molodyk<sup>\*a,b</sup>, Kideok Sim<sup>d</sup>, and Soon Hwang<sup>d</sup>

<sup>a</sup> SuperOx, Moscow, Russia

<sup>b</sup> S-Innovations, Moscow, Russia

<sup>c</sup> Joint institute for High Temperature, Russian Academy of Sciences, Moscow, Russia

<sup>d</sup> SuperGenics Co., Ltd, Changwon, 51542, Korea

(Received 11 November 2019; revised or reviewed 17 December 2019; accepted 18 December 2019)

## Abstract

2G HTS wire with high engineering current density is desired for applications where compact, high power density superconducting equipment is important. We have succeeded in enhancing engineering current density of commercial SuperOx 2G HTS wire based on GdBCO by increasing the HTS layer thickness without fast degradation of the HTS film microstructure. This was possible after improving the temperature uniformity along the HTS film deposition zone. In particular, the wire engineering current density was increased from 700-770 A/mm<sup>2</sup> (for a 65 μm-thick wire without stabilisation) or 430-480 A/mm<sup>2</sup> (for a 105 μm-thick stabilised wire) at the beginning of this study to almost 1200 A/mm<sup>2</sup> (for a 67 μm-thick wire without stabilisation) or 770 A/mm<sup>2</sup> (for a 107 μm-thick stabilised wire) at completion of this study.

*Keywords:* 2G HTS wire, engineering current density, thick HTS layer, HTS film microstructure

## 1. INTRODUCTION

Second generation high temperature superconductor (2G HTS) wire with high engineering current density,  $J_e$ , is required for making compact coils producing high magnetic field for superconducting devices such as rotating machines [1] and various magnets for research facilities [2], particle accelerators [3], future fusion reactors [4, 5], and NMR/MRI machines [6, 7]. One of the ways to increase engineering current density of 2G HTS wire is to increase the HTS layer thickness in the wire. The HTS layer thickness is in the order of one to a few microns, while the total wire thickness is several tens to a few hundred microns. Therefore, this approach increases very slightly the overall conductor cross-section, at the same time the absolute current capacity,  $I_c$ , and hence  $J_e$  may increase from tens to over a hundred percent.

The main obstacle for a potential, if not indefinite but several-fold, increase of  $J_e$  by increasing  $I_c$  with a proportional increase of the HTS layer thickness has been the fast decay of the HTS layer critical current density,  $J_c$ , with thickness and a consequent saturation of  $I_c$  beyond the HTS layer thickness of approximately 1-1.5 microns. The strong  $J_c$  decrease occurs because of the HTS film microstructure degradation, which takes place typically at a thickness above 1 micron [8, 9].

For steady-state HTS film growth experiments, when the stationary substrate is not moving through the deposition zone, the main reason for the degradation of the HTS film microstructure with thickness is believed to be the gradual

decrease of temperature at the growing film surface due to the increase of the HTS film surface emissivity as the surface gets coarser with growth time. Another reason for the cases when the substrate is heated at the bottom via mechanical/thermal contact with a heater surface is, again, the gradual decrease of temperature at the growing film surface because of the deteriorating heat transfer through the thicker HTS film. The effective remedy to extend the microstructure degradation and associated  $J_c$  decrease to higher HTS film thicknesses has been to actively control the substrate heating and optimise the heat/temperature increase with time/growing HTS film thickness.

In 2G HTS wire fabrication, when the substrate tape is moving through the deposition zone, an even more important reason for the HTS film microstructure degradation with increasing thickness is the non-uniformity of growth conditions along the deposition zone, first of all, of deposition temperature. Closed-loop control of temperature profile along the deposition zone using multi-zone heaters enabled, then at a laboratory scale, achieving for the first time an  $I_c$  exceeding 1000 A/cm in a thick HTS film deposited onto a moving buffered Hastelloy substrate tape [9, 10]. Kim et al. reported an  $I_c$  over 1500 A/12 mm in a 5 μm-thick SmBCO film on a 22 m long 2G HTS wire manufactured by a batch co-evaporation process [11]. A recent advance was reported by Selvamanickam and co-workers [12] at a larger, but still pre-commercial production scale: with a modified reel-to-reel MOCVD tool, which incorporated essential upgrades for uniform temperature control, a spectacular HTS film thickness of over 4 μm without significant degradation in

\* Corresponding author: a.molodyk@superox.ru

$J_c$  and microstructure resulting in an  $I_c$  over 1400 A/12 mm was demonstrated.

In this paper we report up to 70% increase of  $J_e$  in production SuperOx 2G HTS wire by increased HTS layer thickness, which, in turn, has been achieved by improved temperature profile in the deposition zone.

## 2. EXPERIMENT

For 2G HTS wire fabrication, standard SuperOx production equipment and processes described in [13, 14] have been used. Briefly, SuperOx 2G HTS wire architecture is based on Hastelloy C276 substrate, IBAD-MgO buffer layer stack terminated with LaMnO<sub>3</sub> cap layer and PLD-GdBCO. For incremental increase of the HTS layer thickness, multiple reel-to-reel depositions have been performed onto the same tape.

The substrate thickness in all wires used in this study was  $60 \pm 3 \mu\text{m}$ . All wires had  $2 \pm 0.5 \mu\text{m}$  of silver deposited on the HTS side and  $1 \pm 0.5 \mu\text{m}$  of silver deposited on the substrate side. HTS thickness varied in the 0.7-4.2  $\mu\text{m}$  range. No stabilising copper layer was used. Therefore, the nominal wire thickness used for calculating wire  $J_e$ , which in our case coincided with non-copper current density,  $J_{nc}$ , was 65-67  $\mu\text{m}$ . For reference, we also calculated wire  $J_e$  assuming typical thickness of stabilising copper layer of 20  $\mu\text{m}$  per side (40  $\mu\text{m}$  overall), or 105-107  $\mu\text{m}$  total wire thickness.

Wire critical current at 77 K has been routinely measured along the entire length in a non-contact mode with a TapeStar XL machine. For each wire, an as-measured TapeStar scan was calibrated with the 4-contact direct transport  $I_c$  measurements with a 1  $\mu\text{V}/\text{cm}$   $I_c$  criterion performed on two or three 1-metre-long sections of that same wire, which had relatively uniform  $I_c$  distribution according to TapeStar data acquired before calibration.

XRD patterns were taken using a Rigaku SamrtLab diffractometer with rotating Cu anode. SEM plan-view images were taken with a Carl Zeiss EVO50 microscope. STEM cross-sectional images were taken with a FEI Tecnai G2 F20 microscope. STEM imaging services were purchased from SMA company [15].

For temperature profile measurements in the PLD chamber, a K-type thermocouple was spot-welded onto Hastelloy transport tape.

## 3. RESULTS AND DISCUSSION

At the beginning of this study, typical production SuperOx 2G HTS wire had an HTS layer thickness of 1.3  $\mu\text{m}$  and an average critical current at 77 K in self-field of 550-600 A/12 mm (Fig. 1), which corresponded to a  $J_c$  of 3.6-3.8 MA/cm<sup>2</sup> and a  $J_e$  of 700-770 A/mm<sup>2</sup> for a 65  $\mu\text{m}$ -thick (0.78 mm<sup>2</sup> cross-section) non-stabilised wire in silver finish only, or, for a 105  $\mu\text{m}$ -thick (1.26 mm<sup>2</sup> cross-section) wire with a typical 20  $\mu\text{m}$  per side copper stabilisation, it would correspond to a  $J_e$  of 430-480 A/mm<sup>2</sup>.

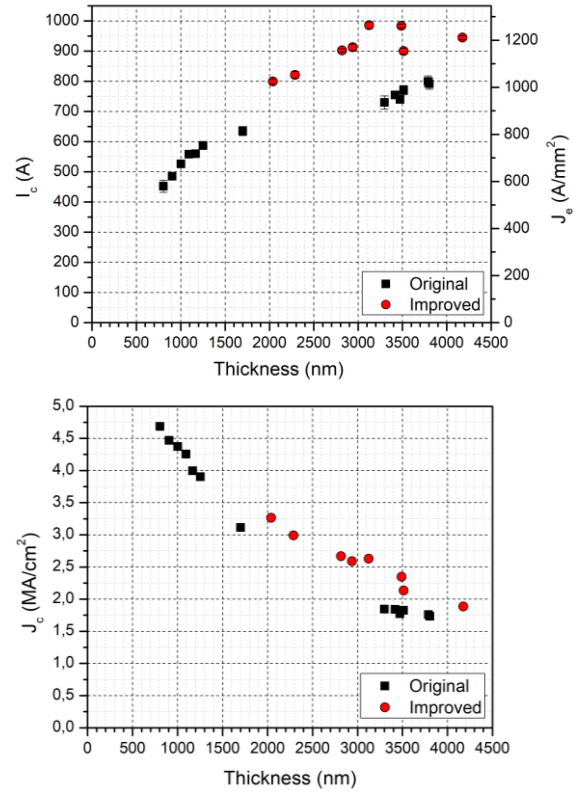


Fig. 1. Dependence on the HTS layer thickness of absolute critical current,  $I_c$ , and engineering current density,  $J_e$ , at 77 K in self-field (top) and critical current density,  $J_c$  (bottom). For wires fabricated with the original temperature profile, at HTS film thickness above 1 micron,  $I_c$  grows with HTS film thickness more slowly than linearly and eventually saturates at a level where no significant  $I_c$  gain can be achieved with further thickness increase. Likewise,  $J_c$  decreases with HTS film thickness. For wires fabricated with improved temperature profile along the deposition zone,  $J_c$  decreases with thickness more slowly, and higher absolute  $I_c$  can be achieved in thick HTS films, up to almost 1000 A in 3-3.5 micron thick films.

With the increase of the HTS layer thickness up to 3.5-3.8  $\mu\text{m}$ , it was possible to achieve an appreciably high absolute critical current of about 800 A/12 mm, which, for the total wire thickness of 67  $\mu\text{m}$ , corresponded to a  $J_e$  of approximately 1000 A/mm<sup>2</sup>, or to 630 A/mm<sup>2</sup> for a 107  $\mu\text{m}$ -thick stabilised wire. As expected, with the increase of the HTS layer thickness, its critical current density decreased, while the absolute critical current saturated and no further significant  $I_c$  gain could be realised with further thickness increase beyond 1.5  $\mu\text{m}$  (Fig. 1). Indeed, with increasing HTS layer thickness gradual deterioration of the HTS layer microstructure took place, which we could detect using SEM (Fig. 2) and XRD (Fig. 3) as the growth of *ab*-oriented and random HTS grains, large secondary phase particles and pores.

Measurement of the temperature profile along the deposition zone revealed a significant variation of temperature, with a span of up to 32°C (Fig. 4). This level of non-uniformity of the HTS layer growth conditions could very well account for the observed deterioration in the HTS film microstructure with increasing thickness.

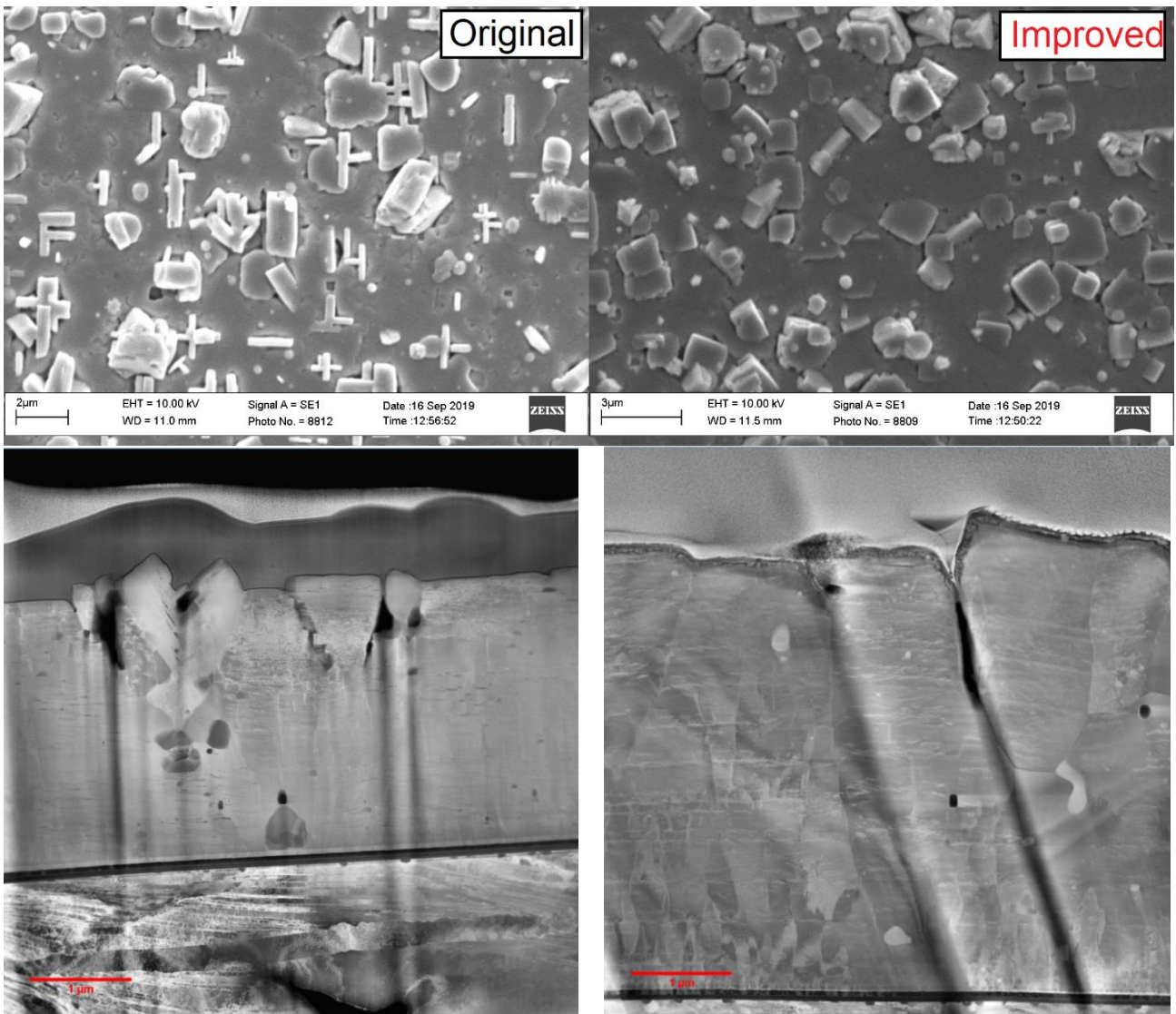


Fig. 2. SEM plan-view (top) and STEM cross-sectional (bottom) images of HTS films fabricated with the original (left) and improved (right) temperature profiles in the deposition zone. Poorer microstructure is observed in HTS films obtained with the original temperature profile: *ab*-oriented and random HTS grains, large secondary phase inclusions and pores are clearly seen in the original HTS films beyond an approximately 1 micron thickness.

In the areas where the temperature was too low, *ab*-oriented and random HTS growth could occur; whereas in the areas with too high temperature, partial decomposition of the HTS phase could occur.

We tried to make the temperature profile in the deposition zone more uniform by re-arranging thermal shields inside the PLD reactor. The exact geometrical configuration of the SuperOx commercial PLD reactor is proprietary and cannot be disclosed in this publication; however, qualitatively, we added more effective shielding near the areas where the tape temperature was lowest. As a result, we could substantially improve the temperature profile uniformity: down to approximately 9°C span within the deposition zone.

With the improved temperature profile, it became possible to extend to higher HTS layer thicknesses the onset of noticeable degradation of the HTS layer microstructure (Fig. 2, 3) and, consequently, higher  $J_c$ ,  $I_c$

and  $J_e$  values were achieved in thick HTS films. Much

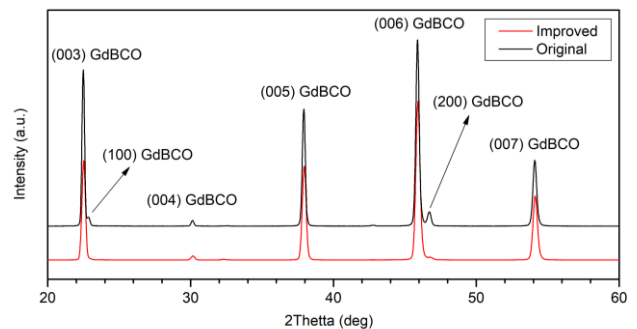


Fig. 3. XRD data of HTS films fabricated with the original and improved temperature profile in the deposition zone. Strong (200) GdBCO peak is present in the XRD patterns of the HTS film fabricated with the original temperature profile.

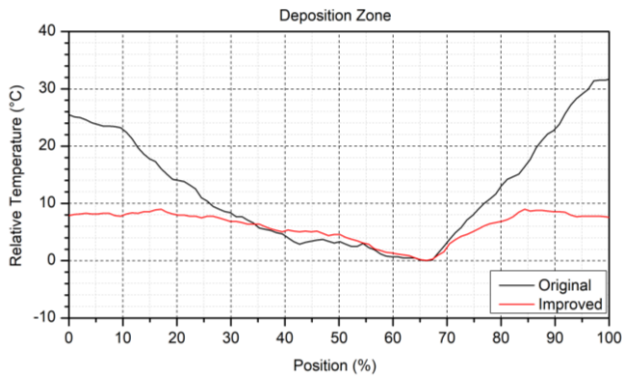


Fig. 4. Temperature profiles along the HTS layer deposition zone measured at the beginning of this study and after improving the arrangement of thermal shields around the deposition zone. In the original temperature profile, the difference between the maximum and minimum temperature within the deposition zone was about 32°C. In the improved temperature profile, the temperature span was reduced to about 9°C.

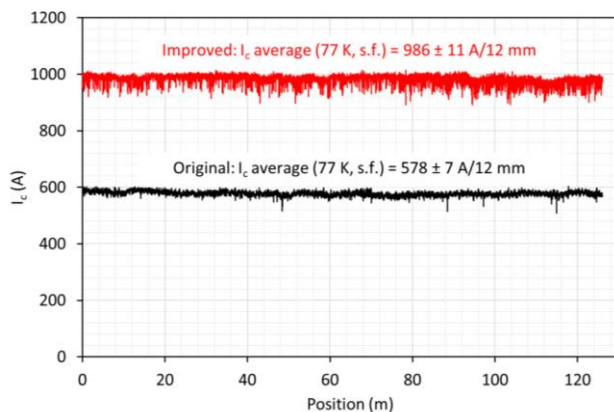


Fig. 5. Positional  $I_c$  (77 K, self-field) data for a 126 m long 2G HTS wire with a 3.1 micron thick HTS layer fabricated with the improved temperature profile. Average  $I_c$  of this wire is  $986 \pm 11$  A/12 mm. For comparison, presented on the plot are also positional  $I_c$  data for a representative wire fabricated at the beginning of this study, with a 1.3 micron thick HTS layer (average  $I_c$  is  $578 \pm 7$  A/12 mm).

smaller (200) GdBCO peak was observed in the XRD patterns, and fewer large microstructure defects were present in the STEM cross-sectional images. Thus, an  $I_c$  of almost 1000 A/12 mm has been demonstrated in 3-3.5  $\mu\text{m}$  thick HTS films (Fig. 1, 5), corresponding to a  $J_e$  of over 1200 A/mm<sup>2</sup> for a 67  $\mu\text{m}$ -thick wire without stabilisation, or to 770 A/mm<sup>2</sup> for a 107  $\mu\text{m}$ -thick stabilised wire.

#### 4. CONCLUSION

We have achieved an approximately 70% increase of engineering current density in commercially produced SuperOx 2G HTS wire by increasing the wire absolute critical current via growing thicker HTS layers. Correspondingly, the increases in  $I_c$  and  $J_e$  at 77 K in self-field were from 550-600 A/12 mm and 700-770 A/mm<sup>2</sup> (for a 65  $\mu\text{m}$ -thick wire without stabilisation) or 430-480

A/mm<sup>2</sup> (for a 105- $\mu\text{m}$ -thick stabilised wire) at the beginning of this study to almost 1000 A/12 mm and 1200 A/mm<sup>2</sup> (for a 67  $\mu\text{m}$ -thick wire without stabilisation) or 770 A/mm<sup>2</sup> (for a 107  $\mu\text{m}$ -thick stabilised wire) as an outcome of this study. This important technological result was possible thanks to improved temperature profile along the HTS film deposition zone, which allowed growing thick HTS layers without significant degradation of the film microstructure.

Further improvement in  $I_c$  and  $J_e$  may be possible by arranging a controlled temperature gradient along the tape path, to compensate for the faster heat loss by the growing HTS film surface due to increasing emissivity with thickness.

At the same time, one has to pay attention to the incremental cost increase of 2G HTS wire with thick HTS layer because of reduced throughput.

#### ACKNOWLEDGEMENT

SuperOx acknowledges the support from Ministry of Science and Higher Education of Russia, Grant 075-11-2018-176 (unique identification number RFMEFI58818X0009).

#### REFERENCES

- [1] <http://asumed.oswald.de/index.php>
- [2] W. D. Markiewicz, et al., "Design of a superconducting 32 T magnet with REBCO high field coils," *IEEE Trans. Appl. Supercond.*, vol. 22, pp. 4300704, 2012.
- [3] J. van Nugteren, et al., "Powering of an HTS dipole insert-magnet operated standalone in helium gas between 5 and 85 K," *Supercond. Sci. Technol.*, vol. 31, no. 6, pp. 065002, 2018.
- [4] Z. Hartwig, "SPARC: The High-field Path to Fusion Energy," presented at ICMC, Hartford, CT, USA, July 21-25, 2019
- [5] G. Brittles, "Stability and quench -dynamic behaviour of Tokamak Energy REBCO QA coils," presented at WAMHTS-5, Budapest, Hungary, 11-13 April 2019, available online at: [https://indico.cern.ch/event/775529/contributions/3334053/attachments/1829923/3003215/20190412\\_GB\\_Stability\\_and\\_quench\\_dyn\\_amic\\_behaviour\\_of\\_Tokamak\\_Energy\\_REBCO\\_QA\\_coils\\_Indico.pdf#search=brittles%20AND%20EventID%3A775529](https://indico.cern.ch/event/775529/contributions/3334053/attachments/1829923/3003215/20190412_GB_Stability_and_quench_dyn_amic_behaviour_of_Tokamak_Energy_REBCO_QA_coils_Indico.pdf#search=brittles%20AND%20EventID%3A775529)
- [6] Y. Iwasa, "HTS and NMR/MRI magnets: Unique features, opportunities, and challenges," *Physica C*, vol. 445, pp. 1088-1094, 2006.
- [7] T. Tosaka, et al., "Project Overview of HTS Magnet for Ultra-high-field MRI System," *Physics Procedia*, vol. 65, pp. 217-220, 2015.
- [8] Q. X. Jia, S. R. Foltyn, P. N. Arendt, and J. F. Smith, "High-temperature superconducting thick films with enhanced supercurrent carrying capability," *Applied Physics Letters*, vol. 80, pp. 1601, 2002.
- [9] S. R. Foltyn, et al., "Materials science challenges for high-temperature superconducting wire," *Nature Mater.*, vol. 6, pp. 631-642, 2007.
- [10] V. Matias and J. Greer, *private communication*, 2011.
- [11] H. Kim, S. Oh, H. Ha, et al., "Ultra-High Performance, High-Temperature Superconducting Wires via Cost-effective, Scalable, Co-evaporation Process," *Sci. Rep.*, vol. 4, pp. 4744, 2015.
- [12] R. Pratap, et al., "Growth of High-Performance Thick Film REBCO Tapes Using Advanced MOCVD," *IEEE Trans. Appl. Supercond.*, vol. 29, no. 5, pp. 6600905, 2019.
- [13] S. Lee, V. Petrykin, A. Molodyk, S. Samoilenov, A. Kaul, A. Vavilov, V. Vysotsky, and S. Fetisov, "Development and production of second generation high Tc superconducting tapes at SuperOx and first tests of model cables," *Supercond. Sci. Technol.*, vol. 27, no. 4, pp. 044022, 2014.

- [14] S. Samoilenkov, A. Molodyk, S. Lee, V. Petrykin, V. Kalitka, I. Martynova, A. Makarevich, A. Markelov, M. Moyzykh, and A. Blednov, "Customised 2G HTS wire for applications," *Supercond. Sci. Technol.*, vol. 29, pp. 024001, 2016.
- [15] <https://www.microscop.ru/>